

OEP (Opto Electronic Processor) for Extremely Fast Multi-Channel Analog and Digital OE-Signal-Processing

R. Schwarte, Z. Zhang, M. Grothof, J. Frey, H. Kraft, T. Moeller, H. Hess, Universität Siegen;
B. Buxbaum, T. Ringbeck, Z. Xu, PMDTechnologies GmbH / S-TEC GmbH, Siegen

Universität Siegen
Institut für Nachrichtenverarbeitung (INV)
Hölderlinstraße 3
57068 Siegen

PMDTechnologies GmbH
Am Eichenhang 50
57076 Siegen

1. ABSTRACT AND INTRODUCTION

Optoelectronics and photonics become key technologies more and more, being particularly the most ambitious and innovative technologies in communications and sensor techniques, automation and safety. In this context there is a lasting demand for improvements in order to fasten and to simplify opto-electronic processing and interconnection techniques as well as photonic measurement techniques.

This paper presents new procedures and components for low cost and high speed optoelectronic analog and digital signal processing and interfacing. Following examples demonstrate new capabilities of multi-channel light processing and measurement performing low noise, high dynamics, pico-second time resolution, high sensitivity and electronically controlled pure optical signal processing.

A new component **PMD (Photonic Mixer Device)** introduced an advantageous standard into fast 3D-imaging by applying a detector-inherent mixing and correlation process [1,2,3]. Meanwhile the PMD technology achieved a mature state, e.g. enabling frame rates of 100 3D-images at 256 PMD-pixels per second. The University of Siegen Institutes INV and ZESS and the Siegen firms PMDTechnologies and S-TEC GmbH are looking forward to a road map of increasing pixel numbers to more than 10.000 PMD-pixel (look at paper 4.2 in this OPTO 2004 proceedings). In parallel to this way we developed new similar photonic technology as exciting as the PMD-technology: We found that a PMD-combination, i.e. OE-integrated components using the inherently mixing and switching PMD-principle, is ideally suited for new high speed analog and digital optoelectronic signal processing capabilities. This new device is called **OEP Opto-Electronic Processor**. It is composed of PMD-structures in Schottky technology [4,5,6] and will offer an extraordinary high bandwidth or bit rate in the 10 to 30 GHz / Gbit/s - range.

Schottky-PMD technology in GaAs- or silicon enables this extremely high speed based on the Schottky-MSM (Metal Semiconductor Metal)-Photodiode which is known to enable a bandwidth of more than 100 GHz [3].

2. PRINCIPLE OF OPERATION AND OE-CORRELATION PERFORMANCE OF THE MSM-PMD

Figure 1 illustrates the cross section of the MSM-photodiode including the simplified circuitry for the MSM-PMD functionality.

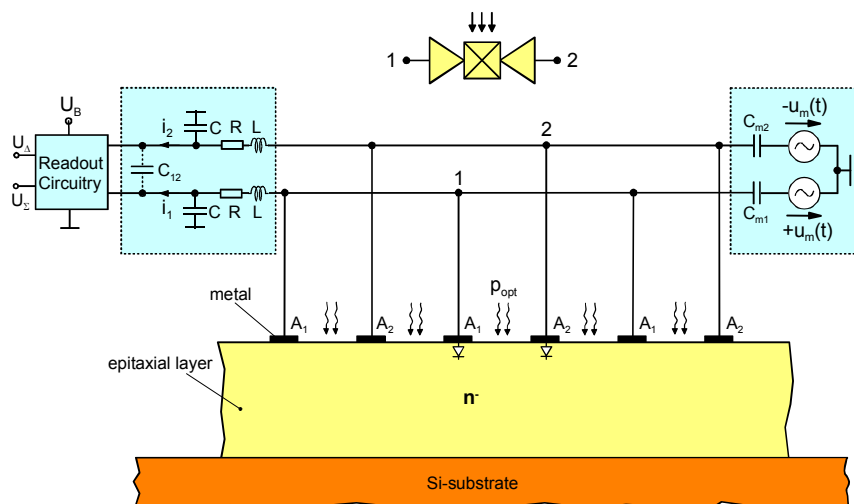
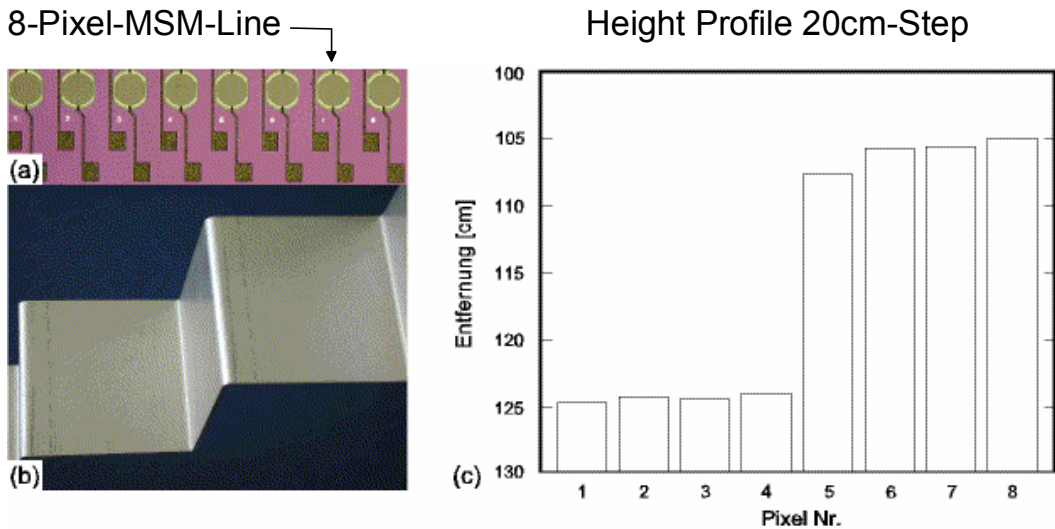


Figure 1: Cross section of the MSM-PMD with simplified circuitry



Distance Measurement with a MSM-PMD-Sensor Line:
 Standard Deviation R ca. 2mm @ $f_{\text{mod}} = 20 \text{ MHz}$

Figure 2: MSM-PMD line measuring a spatial step profile

The finger structure sequence for instance shows $1\mu\text{m}$ Metal, $2\mu\text{m}$ Semiconductor gap, $1\mu\text{m}$ Metal and so on, e.g., on a low doped GaAs-epitaxial layer. **Figure 3** shows the equivalent top view of two of those MSM-structures. Connections 1 and 2 “see” a minimum of two anti-serial Schottky diodes, one is forward biased and the other is reverse biased due to the voltage polarity. Photo charge is produced in the photosensitive gap between the metal stripes, more precise in the space charge region of the actually reverse biased Schottky diode. Thus the readout current polarity is multiplied by the voltage polarity. If the illumination $P_{\text{opt}}(t)$ correlates with the voltage $\pm u_m(t)$ we get a high selective correlation result respectively measurement result after an appropriated current integration time. For balanced modulation and non correlated illumination like sunshine there is no charge out of balance, ideally producing no disturbing signal. This special characteristic leads to extremely high background light suppression and high sensitivity. The experimental result in **Figure 2** demonstrates the high time resolution, stability, sensitivity and correlation performance of the MSM-PMD, proved by means of an 8-pixel MSM-PMD-array in a laserradar-receiver measuring a spatial step profile of **20mm** height. It exhibits a standard deviation of less than **2mm**, respectively about 10ps time-of-flight, at a light-modulation and PMD-demodulation frequency of 20 MHz.

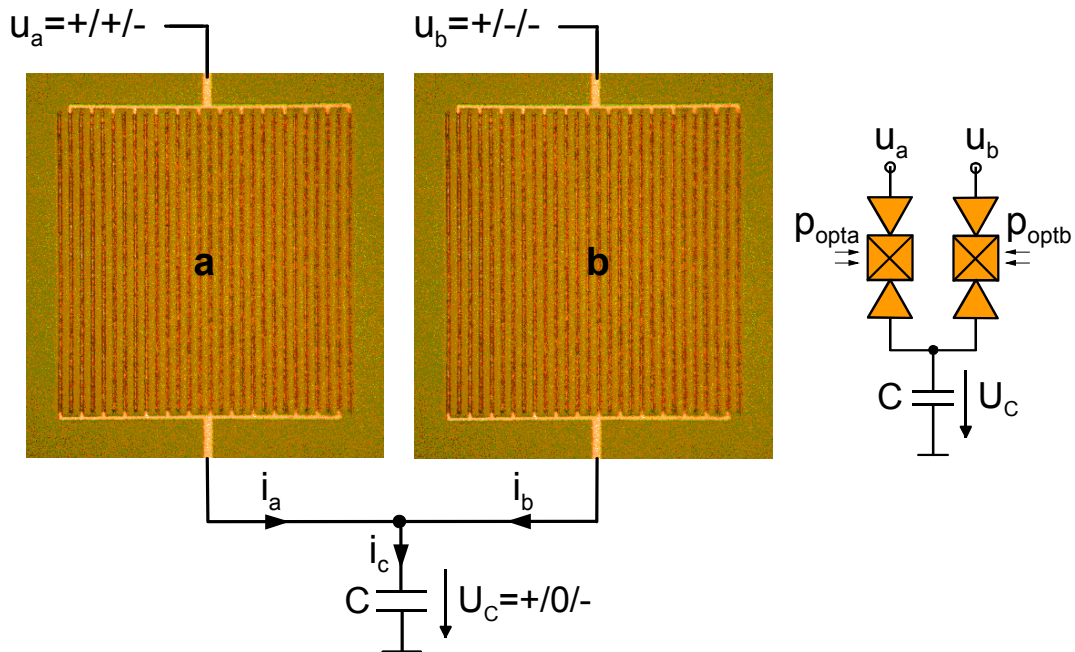


Figure 3: Basic OEP-principle formed by two MSM-PMDs

3. PRINCIPLE OF OPERATION AND BASIC STRUCTURES OF THE OEP (OPTO ELECTRONIC PROCESSOR)

In the simplest case two PMDs are connected on one side and form an OEP by summarizing their photocurrents as shown in **Figure 3**. Here we assume the same photon flux $P_{opta} = P_{optb}$ to each pixel. New functionalities are generated by individual controlling of the two photocurrents by means of the voltages u_a and u_b . For the sake of clarity we consider three special cases at constant and equally balanced illumination:

- 1) For positive even voltages $u_a = u_b$ we get a total current $i_c = i_a + i_b$ and a positive sensitivity.
- 2) For odd voltages $u_a = -u_b$ we get $i_c = i_a + i_b = 0$, a zero sensitivity. We don't get any charge on the capacity C. This is an surprising characteristic of the OEP providing a novel photodetector which can be switched off extremely fast and simple.
- 3) For negative even voltages the negative photocurrents are summarized to a negative sensitivity.

Between these extreme points of operation the device offers a total range of controlled photosensitivity from -100% to +100%. At a first glance these capabilities look unimpressive. But they really open a wide range of new solutions especially at high speed.

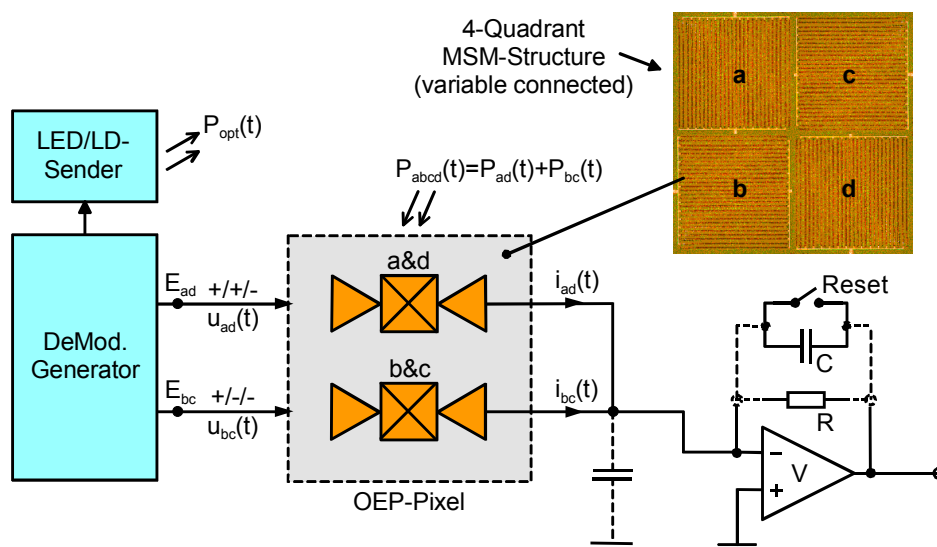


Figure 4: 4-Quadrant MSM-OEP, a multi-functional programmable PMD combination

The right side of **Figure 3** depicts the equivalent circuit of this OEP. This OEP-circuit with the capacity C suggests to anticipate an operation as an optical sampler of $P_{opt} = P_{opta} + P_{optb}$. In the non-sampling state two conditions have to be fulfilled, $u_a = -u_b$ and $P_{opta} = P_{optb}$. For getting an e.g. positive sampling probe the negative $u_b(t)$ has to be switched to the positive voltage level for the period of sampling time. This OEP-application is more detailed investigated in **Figure 5**.

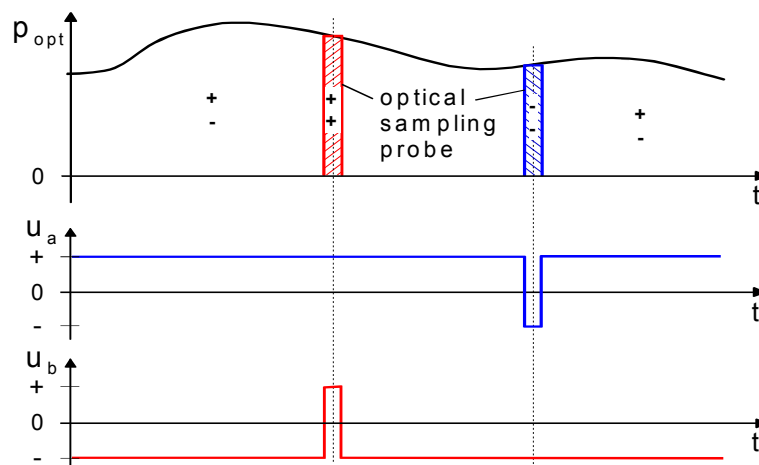


Figure 5: Illustration of optical bipolar OEP-sampling process

In order to assure an almost equal optical power distribution of P_{opt} we apply a 4-Quadrant structure of this two-pixel OEP as shown in Figure 4 in top view. Here the diagonal quadrants a&d in **Figure 4** stand for the PMD- pixel a of **Figure 3** while quadrants b&c are standing for the PMD-pixel b.

Before describing OEP-facilities by some examples and applications we summarize the main functionality: the OEP-output current i_c of a minimum two pixel-OEP in **Figure 3** is a function of the two controlling optical signals P_a and P_b and of the two controlling voltages u_a and u_b . OEPs are totally controlled photodetectors but they also can be reduced to pure PMD-functionality by parallel connection of all PMDs included.

4. NEW OE-SOLUTIONS AND OE- APPLICATIONS ENABLED BY OEP

In **Figure 4** a 4-quadrant OEP is shown in top view together with its equivalent circuit symbol. Here it serves as an one-pixel OEP with one output of total current $i_A = i_{ad} + i_{bc}$. It is composed of two PMDs a&d and b&c which are composed of diagonally placed areas with orthogonally lined finger structures providing an optimal balanced optical power distribution of $P_{abcd}(t) = P_{opt}$ and rf-decoupling. This device is ideally appropriated e.g. for a fast optical sampling process as illustrated in **Figure 5**.

Here the incident optical signal P_{opt} is ignored as long as the voltages are balanced at $u_a = -u_b$ and marked by the "+ - region". At the scheduled trigger point for a positive sampling probe the negative voltage u_b is switched from minus to plus during a minimum sampling time of some 10 ps ("++ region") provided sufficient incident optical power. For a negative sampling probe u_a is switched from plus to minus in the "-- region". This operation realizes a picosecond-3D-stroboscope.

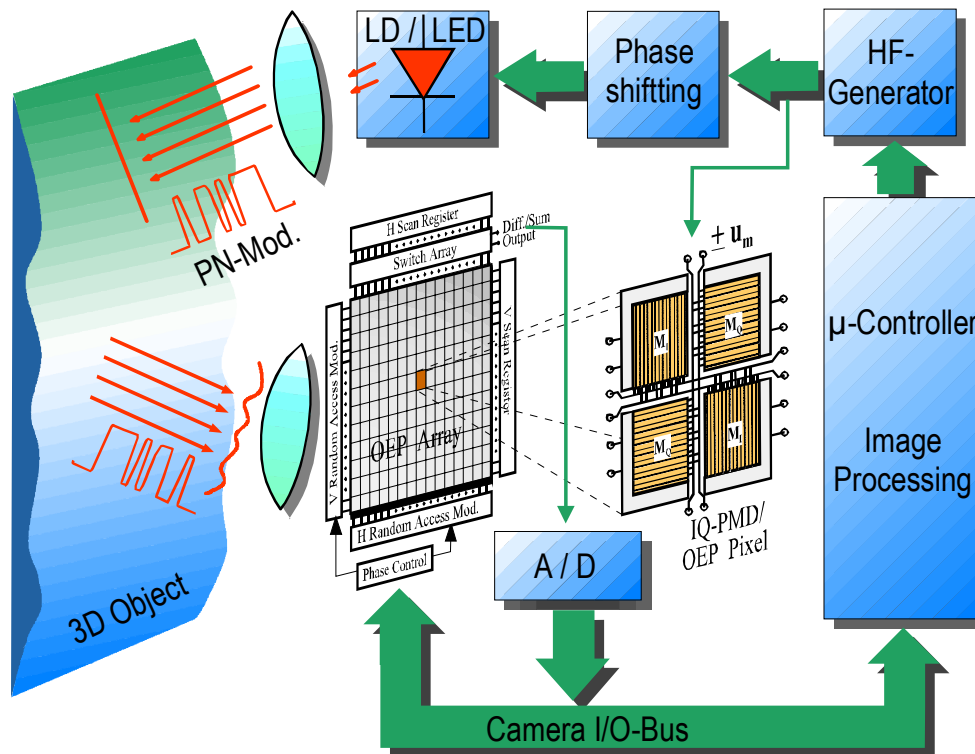


Figure 6: Block diagram and principle of operation of 3D-PMD- and 3D-OEP-camera

Alternatively the one-output MSM-structure in **Figure 4** could be operated with two outputs as a 2-pixel OEP with OEP a&d and OEP b&c for a demultiplexing process into two channels or as a two simultaneously operating IQ(90°/0°)-PMDs. A first suggested application as depicted **Figure 4** is an OEP-laser-radar comprising a modulation generator for modulating the LED/laserdiode sender and for demodulating the reflected optical signal $P_{abcd}(t)$ by means of the 1-pixel OEP receiver which applies charge readout. Distances are measured by evaluating the echo-TOF (time-of-flight). Using an array of OEP-pixel enables 3D-imaging by a 3D-OEP-camera in **Figure 6** like a 3D-PMD-camera but with some advantages. The main progress of a new 3D-OEP-camera is the possibility of burst, 3D-digital storage and 3D-sampling operation, further the extremely short sampling time down to some 10 to 100 ps and the background light suppression. This TOF-sampling procedure is quite similar to the electronic TDR (Time Domain Reflectometry)-operation

of sampling oscilloscopes for repetitive signals or to the electronic DSO (Digital Storage Oscilloscope)-measurements of single events. In the case of 3D-optical sampling the total 3D-scene respectively the volume signal is captured.

We suppose the OEP-technology is of utmost importance for OE-switching technologies.

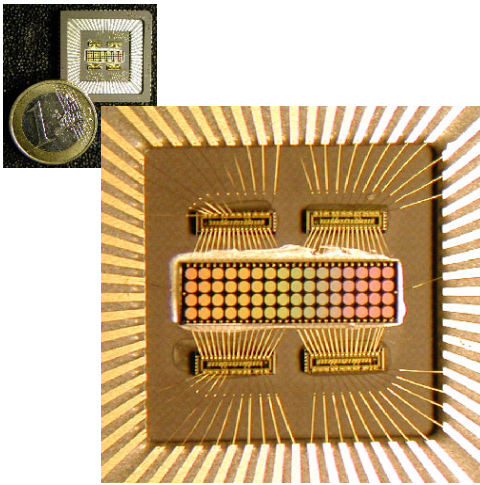


Figure 7: Chip photo of a 64 pixel MSM-PMD/OEP array

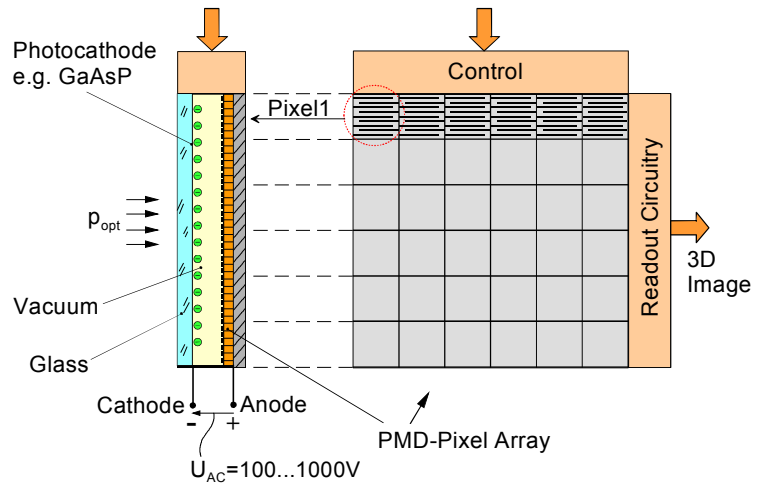


Figure 8: MSM-PMD/OEP array with image intensifier

Figure 7 shows a chip photo of a 64 pixel MSM-PMD/OEP-array providing a great number of exciting applications using multi-chip technology.

Figure 8 shows an OEP-improvement to higher sensitivity by about 1000fold electron-energy amplification in vacuum. The photoelectrons behind the photocathode are accelerated by an adjustable negative cathode potential of 100 to 1000 volts. The MSM-structures are bombarded with high-energy electrons of about 1000 eV instead of photons of about 1 to 2 eV which results in an about 1000fold photo charge. In praxis the range of such a laser-radar can be increased to more than one km.

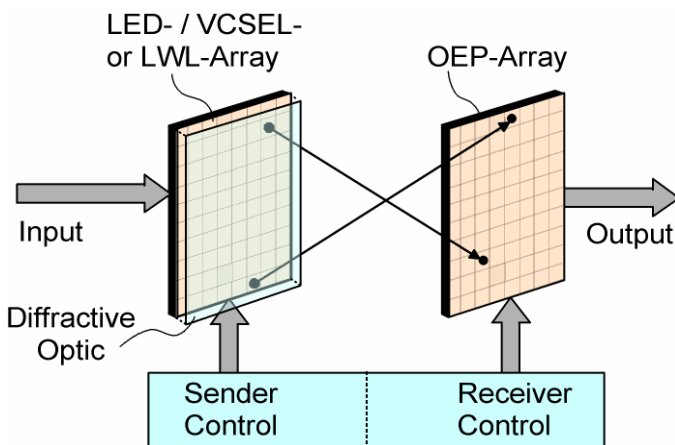


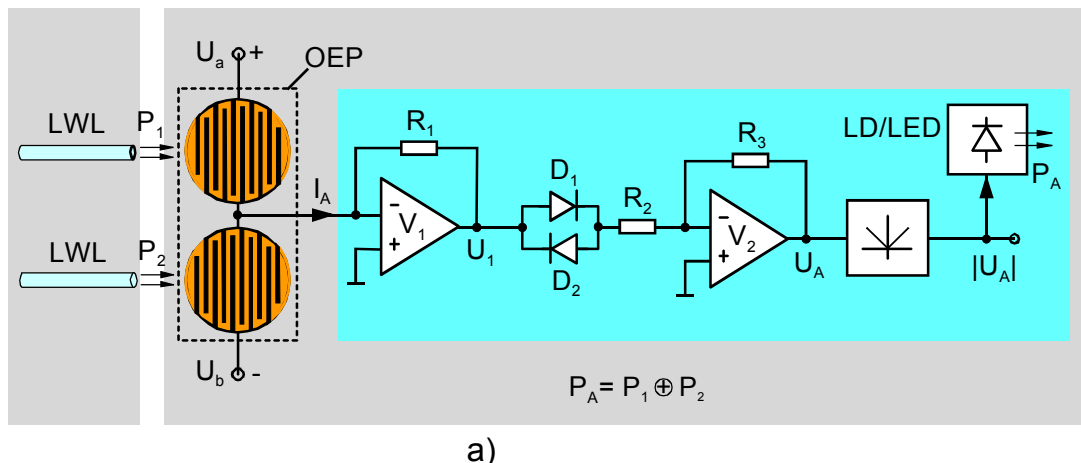
Figure 9: Optical cross connect and router using LED/LD- and OEP-array

Figure 9 demonstrates a cross connect and router configuration providing a high switching capacity solution of flexible size and low-cost. The LED/VCSEL-Array or LWL-bundle is optically connected to an array of OEP-receivers. The connecting volume may be reduced e.g. to the size of an IC-package or enlarged to big rooms as well for flexible interconnection as for communications. Channel allocation is performed by means of code-, code-phase- and time multiplexing.

As shown in **Figure 10b** this XOR-function has been proved by an experimental setup using LEDs in the range from kilobit/s to about 100Mbit/s: $P_A = P_1 \oplus P_2$.

One example in **Figure 10** demonstrates the digital facilities of OEP-arrays for OE-interfacing. The OE-circuit in **Figure 10a** provides a pure optical XOR-functionality of the two optical inputs P_1 and P_2 to the optical LED- or laser output $P_A = P_1 \oplus P_2$. The electronic circuit amidst is an extremely small CMOS-

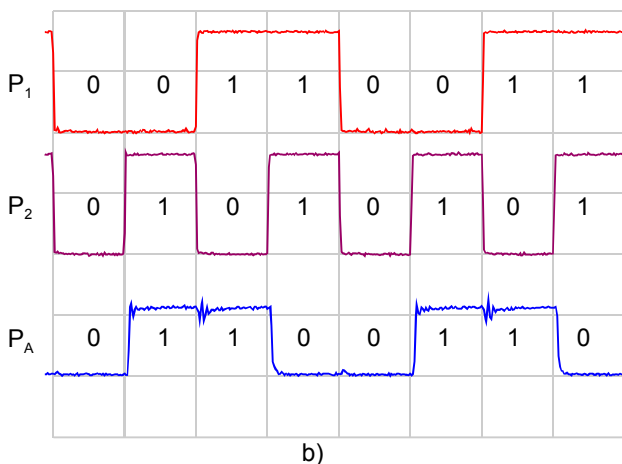
A further digital function is still simpler: For instance we want to readout pure optically the 16 bit parallel bus states of a memory. The explanation starts with **Figure 10a**. Now each OEP is connected to only one fiber providing optical readout pulses $P_{in} = P_1 + P_2$ equally distributed. The digital memory states are connected to the U_b -clamps while U_a stays positive. The logical state of U_1 is connected to the LD / LED via an inverter. The result is $P_A = U_b \text{ AND } P_{in}$, i.e., only for memory states $U_b = \text{HIGH}$ the optical output P_A reacts with a pulse to an optical readout pulse P_{in} .



a)

Figure 10a): Pure optical XOR based on OEP and LED/Laser diode

Harnessing these different capabilities of OEP- and PMD-structures within arrays for sensing and capturing space and time this technology enables – besides 3D-Imaging as shown in **Figure 6** – a broad spectrum of new solutions:



b)

Figure 10b): Experimental result of pure optical XOR-realisation using LEDs in the kHz to 100Mb/s-range

- Multi-channel-3D-Sampling
- Direct capturing of the 3D-optical flow e.g. due to robotic and automotive movements by simultaneously analyzing the radial increments for radial speed and the lateral space frequency for lateral speed (including speed-over-ground)
- Large range and high sensitivity due to burst operation causing higher power level and RF-CBS (Correlated Balanced Sampling)
- Multi-channel analog and digital OE-signal processing and demultiplexing techniques for fast ADCs e.g. by dividing PMD-pixels in N-sectors for realizing a N/2-OEP-DeMux.
- Multi-channel free-space and fiber-optical Code/Time/Phase-Domain Multiplex for communications and interconnection.

CONCLUSION AND ACKNOWLEDGEMENT

This paper provides an introduction to the exciting facilities of the OEP-technology which is derived from the PMD-technology in order to attain new optoelectronic solutions and applications. For our opinion OEP will become a key component for the photonic world. Thanks to all coworkers of the INV-, PMDTechnology-, S-TEC- and ZESS-teams for their engaged cooperation.

REFERENCES

1. Z. Xu: Investigation of 3D-Imaging Systems Based on Modulated Light and Optical RF-Interferometry (ORFI), ZESS Forschungsberichte, Shaker-Verlag, ISBN 3-8265-6726-6, Aachen 1999.
2. B. Buxbaum: Optische Laufzeitentfernungsmessung und CDMA auf Basis der PMD-Technologie mittels phasenvariabler PN-Modulation, ZESS Forschungsberichte, Shaker-Verlag, ISBN 3-8265-9805-9, Aachen 2001.
3. T. Ringbeck: Untersuchung opto-elektrischer Phasenregelkreise auf Basis von Photomischdetektoren hinsichtlich deren Anwendungspotential für die Photonik, ZESS Forschungsberichte, Shaker-Verlag, ISBN 3-8265-9789-3, Aachen 2001.
4. R. Schwarte: Dynamic 3D-Vision. EDMO 2001, Wien
5. R. Schwarte: Miniatur-3D-Kamera für mobile Telerobotik und Telemanipulation. Telerobotik-Konferenz, Siegen, Juni 2003.
6. Z. Zhang: Untersuchung und Charakterisierung von PMD (Photomischdetektor)-Strukturen und ihren Grundschaltungen. Doctoral thesis, University of Siegen, to be published, 2003